CrossMark

Capillarity-Driven Oil Flow in Nanopores: Darcy Scale Analysis of Lucas–Washburn Imbibition Dynamics

Simon Gruener[1] · Patrick Huber[2]

Abstract

We present gravimetrical and optical imaging experiments on the capillary-driven imbibition of silicone oils in monolithic silica glasses traversed by 3D networks of pores (mesoporous Vycor glass with 6.5 nm or 10 nm pore diameters). As evidenced by a robust square root of time Lucas–Washburn (L–W) filling kinetics, the capillary rise is governed by a balance of capillarity and viscous drag forces in the absence of inertia and gravitational effects over the entire experimental times studied, ranging from a few seconds up to 10 days. A video on the infiltration process corroborates a collective pore filling as well as pronounced imbibition front broadening resulting from the capillarity and permeability disorder, typical of Vycor glasses. The transport process is analyzed within a Darcy scale description, considering a generalized prefactor of the L–W law, termed Lucas–Washburn–Darcy imbibition ability. It assumes a Hagen–Poiseuille velocity profile in the pores and depends on the porosity, the mean pore diameter, the tortuosity and the velocity slip length and thus on the effective hydraulic pore diameter. For both matrices a reduced imbibition speed and thus reduced imbibition ability, compared to the one assuming the nominal pore diameter, bulk fluidity and bulk capillarity, can be quantitatively traced to an immobile, pore wall adsorbed boundary layer of 1.4 nm thickness. Presumably, it consists of a monolayer of water molecules adsorbed on the hydrophilic pore walls covered by a monolayer of flat-laying silicone oil molecules. Our study highlights the importance of immobile nanoscopic boundary layers on the flow in tight oil reservoirs as well as the validity of the Darcy scale description for transport in mesoporous media.

Keywords Imbibition · Silicone oil · Mesoporous silica · Nanoporous media · Darcy law

✉ Patrick Huber
  patrick.huber@tuhh.de

  Simon Gruener
  simon-alexander.gruener@basf.com

1 Sorption and Permeation Laboratory, BASF SE, 67056 Ludwigshafen, Germany

2 Institute of Materials Physics and Technology, Hamburg University of Technology, 21073 Hamburg-Harburg, Germany

    Springer

1 Introduction

Fluid transport in pores a few nanometers across is of relevance in many natural and technological processes (Eijkel and Berg 2005; Stone et al. 2004; Squires and Quake 2005; Schoch et al. 2008; Kirby 2010), ranging from water transport in soils (Alyafei et al. 2016; Bao et al. 2017), plants (Stroock et al. 2014; Zhou et al. 2018) and biomembranes (Zhang et al. 2018b) to water filtration, catalysis (Montemore et al. 2017), print (Kuijpers et al. 2018) and Lab-on-a-Chip (Piruska et al. 2010; Li and Seker 2017) technologies. It is also of increasing importance in the synthesis of hybrid materials (Sousa et al. 2014; Martin et al. 2014; Busch et al. 2017) by melt-infiltration (Jongh and Eggenhuisen 2013). In particular, self-propelled, capillarity-driven imbibition in nanoporous media plays a dominant role in many petrophysical processes, ranging from the mass transfer in fractured reservoirs during a waterflood to wettability characterization of rock samples and geothermal reservoirs (Schmid and Geiger 2013; Huber 2015; Meng et al. 2017; Yang et al. 2017; Zhang et al. 2018a).

The advent of tailorable nanoporous materials, most prominently based on carbon (Holt et al. 2006), silicon (Vincent et al. 2017; Gruener and Huber 2008), gold (Xue et al. 2014), silica with sponge-like (Gruener et al. 2009; Kelly et al. 2018; Kiepsch and Pelster 2016; Gruener et al. 2012) and regular pore geometry (Persson et al. 2007; Sentker et al. 2018), and alumina (Shin et al. 2007; Koklu et al. 2017; Yao et al. 2017) provides model porous media in order to study this phenomenology in well-defined spatial confinement (Kriel et al. 2014).

Because of the extreme spatial restrictions in nanopores the validity of continuum hydrodynamics is questionable, both with regard to the coarse-graining procedure as well as the correctness of the standard no-slip velocity boundary condition at the pore wall (Falk et al. 2015). The details of the velocity profile in the proximity of the confining walls sensitively determine the overall transport rates. The "no-slip at the wall" concept is considered to hold for a single-component fluid, a wetted surface, and low levels of shear stress (Bocquet and Tabeling 2014). In many engineering applications these conditions are not met (Stone et al. 2004). Both experimental and theoretical studies have revealed that slippage, that is a finite velocity of the liquid at the wall can occur in systems with surfactants, at high shear rates, low roughnesses of the confining walls as well as crystalline wall structures incommensurable with adsorbed monolayers of the respective liquid (Thompson and Troian 1997; Cieplak et al. 2001; Schmatko et al. 2005; Neto et al. 2005; Servantie and Mueller 2008; Sendner et al. 2009; Baeumchen et al. 2012; Ortiz-Young et al. 2013; Bocquet and Tabeling 2014; Gruener et al. 2016a; Secchi et al. 2016).

Moreover, liquids slipping at a substrate are observed in non-wetting configurations (Vinogradova 1999; Lasne et al. 2008; Barrat and Bocquet 1999; Baeumchen et al. 2012; Gruener et al. 2016b; Wu et al. 2017a; Meng et al. 2017). Also applying chain-like or more generally spoken polymeric fluids seems to facilitate the occurrence of slip at the fluid–solid interface (Dimitrov et al. 2007; Gruener et al. 2016a).

The first experiments to explore flow behavior through mesoporous glasses were performed by Nordberg (1944), and Debye and Cleland (1959) in the mid of the last century. For liquid hydrocarbons flow rates in agreement with the classical Hagen–Poiseuille prediction for simple capillaries were observed, if an adsorbed layer of molecular thickness at the wall is considered in the transport process. By contrast, for even smaller pores, below 2 nm, as typical for kerogen transport in shales, a breakdown of classical hydrodynamic concepts, in particular the Darcy scale description as a generalization of the Hagen–Poiseuille law toward viscous flows in complex pore networks is expected (Falk et al. 2015).
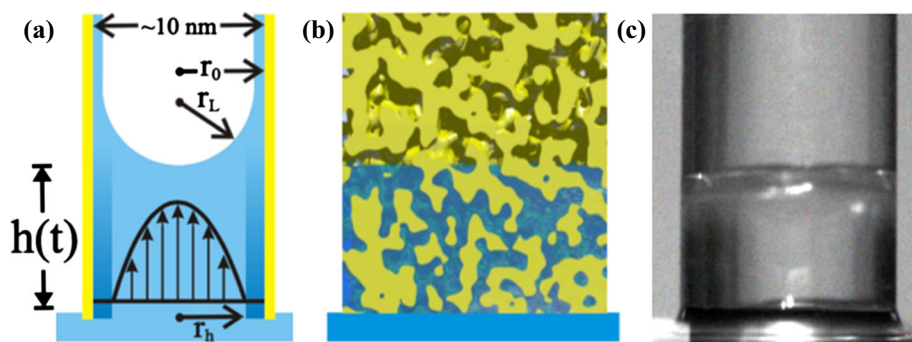
Fig. 1 Capillary Rise of Oil in Nanopores. **a** Illustration of capillarity-driven liquid imbibition in a cylindrical capillary with a preadsorbed water layer. The fluid has advanced up to the height $h(t)$ and a parabolic velocity profile developed while a boundary layer (shaded region) remains at rest. The different radii are discussed in the text. **b** Raytracing side-view on spontaneous imbibition in a Vycor monolith, which is represented by a clipped Gaussian random-field. **c** Picture of a V5 Vycor rod in which a silicone oil imbibition front has advanced up to a height $h(t) = 5$ mm. See also a video on the imbibition process in the supplementary

Depending on the relative size of the pores and the basic building blocks of the liquid, the temperature and the pressure of the fluid, transport in porous media can be governed by a complex interplay of adsorption processes, Knudsen, (Gruener and Huber 2008; Kiepsch and Pelster 2016; Wang et al. 2016), Fickian and surface diffusion (Yamashita and Daiguji 2015), as well as viscous liquid flow driven by capillarity ("spontaneous imbibition") or by hydraulic pressure ("forced imbibition") (Gruener et al. 2016b; Vincent et al. 2017).

We focus here on spontaneous imbibition in porous silica monoliths with pore diameters of 6.5 and 10 nm and thus in the lower "mesoporous" regime. Previous studies on the flow of water (Huber et al. 2007; Gruener and Huber 2009; Gruener et al. 2016b), and of linear hydrocarbons (Gruener et al. 2009, 2016a) in such porous glasses revealed a retained fluidity and capillarity compared to the bulk liquids, if a sticky molecular boundary layer is assumed at the pore walls. It results in a slow-down of the imbibition dynamics. In this study, we extend our previous spontaneous imbibition studies on simple liquids toward slightly more complex molecules, i.e., silicone oils. We perform gravimetrical experiments and analyze the scaling of the measured imbibition kinetics based on a Darcy effective medium ansatz.

2 Materials and Methods

2.1 Porous Glass Substrates

Nanoporous glass samples were purchased from Corning glass (Vycor glass, code 7930). Vycor is virtually pure fused silica glass permeated by a three-dimensional network of interconnected pores (Levitz et al. 1991; Huber and Knorr 1999). It is formed by a leaching process after spinodal decomposition of a borosilicate glass. Therefore, its geometric structure can be well represented by Gaussian random-fields (Gommes 2018), see Fig. 1 for a raytracing illustration of the Vycor structure. The experiments were performed with two types of Vycor with identical porosity $\phi_0 \approx 0.3$ and differing mean pore radius $\bar{r}_0$. The two types will be termed V5 ($\bar{r}_0 = 3.4\ nm$, $\phi_0 = 0.315 \pm 0.005$) and V10 ($\bar{r}_0 = 5.0\ nm$, $\phi_0 = 0.3 \pm 0.005$) in the following. The characterization of the matrix properties, in particular $\bar{r}_0$, relies on volumetric nitrogen sorption isotherms performed at 77 K (Gruener et al. 2016a).
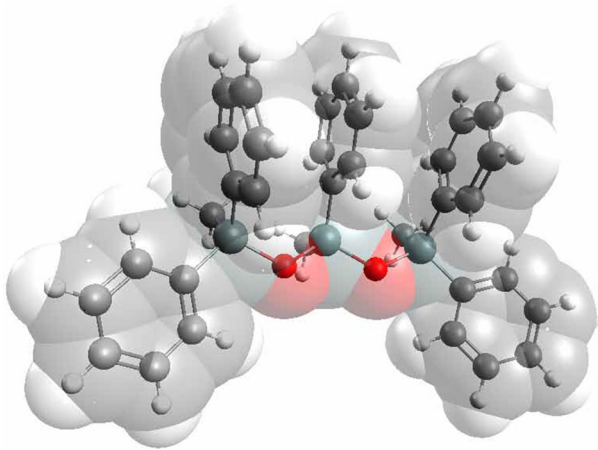
Fig. 2 Molecular structure of silicone oil. Illustration of the molecular structure of 1,1,3,5,5-Pentaphenyl-1,3,5-trimethyltrisiloxane. It is the main constituent of the Dow Corning diffusion pump oils DC704 and DC705. Five phenyl and three methyl groups are regularly attached to the trisiloxane ($Si_3O_2 - R_8$) backbone. The molecular dimensions can roughly be estimated using the diameter of a phenyl ring ($\sim 5.4\,\text{Å}$) to be between 1 nm and 1.5 nm (Gruener 2010)

The relatively low porosity along with the high elastic modulus of the silica glass renders any liquid uptake-induced mechanical deformation negligible (Gor et al. 2017, 2018), in the sub-percent range. Any impact of swelling or contraction, which in principle could affect the imbibition process significantly (Kvick et al. 2017) can thus be ignored.

We cut regularly shaped cylinders and blocks of height d ($\sim$ 10 mm) from the delivered rods. To remove any organic contamination, we subjected them to a cleaning procedure with hydrogen peroxide and nitric acid followed by rinsing in deionized Millipore water and drying at 200 °C in vacuum for two days. The pore walls of Vycor are polar due to a silanol termination. This hydroxylation renders these matrices highly hydrophilic (Gruener et al. 2009).

2.2 Silicone Oils

As oily model liquids we employed the diffusion pump oils DC704 and DC705 from Dow Corning. Their main building blocks are siloxane molecules, see Fig. 2 and exhibit a negligible vapor pressure and a relatively high viscosity (see Table 1) (Gruener 2010).

2.3 Experimental

The capillary rise dynamics of the silicone oils have been recorded gravimetrically and by means of a CCD monochrome camera placed in front of the imbibition setup. The imbibition dynamics can be tracked by recording the increase in the sample's mass due to liquid uptake (Gruener 2010; Gruener and Huber 2011; Gruener et al. 2016a). Such experiments can be easily performed by means of a laboratory scale. The sample is attached to the balance allowing time-dependent recording of the gravitational force acting on the porous block—see inset in Fig. 3 for an illustration.

Table 1 Fluid properties: Dow Corning silicone oils at $T = 25\,°C$. The values are taken from pycnometer and rheometer measurements as well as from Wohlfarth and Wohlfarth (1997)

DC	Density ρ (g/ml)	Viscosity η (mPa s)	Surface tension σ (mN/m)
704	1.0772	48.99	32.85
705	1.1033	218.8	35.24

3 Darcy Analysis of Liquid Imbibition in a Hydrophilic Nanoporous Medium

In the following, we outline a phenomenological treatment of the capillary rise in a porous medium, as described in detail in Gruener et al. (2016a), Gruener (2010). It assumes that both gravitational and inertial affects are negligible compared to the huge capillary forces in the nanopores. However, the model considers changes in the available volume porosity for imbibition ϕ_i compared to the nominal porosity of the sample ϕ_0, as determined after bake-out in vacuum, since during the imbibition process pore space is occupied by preadsorbed water and hence no longer available. The exact value of the initial porosity ϕ_i is accessible by an analysis of the overall mass uptake of the sample.

Moreover, the resulting changes in the curvature radius of the concave liquid menisci in the pores are considered as well as an effective hydraulic pore diameter r_h. This diameter does not necessarily have to agree with the pore radius r_0, determined by the sorption isotherm measurements of the baked-out sample, because of either strongly adsorbed, immobile boundary layers and thus a negative velocity slip length b ($r_h < r_0$, i.e., $r_h = r_0 + b$) (Gruener and Huber 2011), or due to velocity slippage at the pore walls ($r_h > r_0$) (Gruener et al. 2009; Gruener and Huber 2009; Vo et al. 2015; Vincent et al. 2016; Shen et al. 2018). Only for the standard no-slip boundary condition is $r_h \equiv r_0$. Note that r_h coincides with the radius over which a parabolic flow profile is established in the pore—see Fig. 1a.

Neglecting the initial ballistic imbibition regime (Kornev and Neimark 2001), which can be estimated to last just a few ps, we focus on the regime of viscous flow, where viscous dissipation prevails and acts against the capillarity-driven liquid uptake by the porous medium (Bell and Cameron 1906; Lucas 1918; Washburn 1921; Rideal 1922). The competition of the constant Young-Laplace driving pressure and the increasing viscous drag in the liquid column behind the advancing imbibition front results in the Lucas–Washburn–Darcy $\sqrt{t}$ law for the rise height $h(t)$ (Lucas 1918; Washburn 1921; Rideal 1922)

$$h(t) = \sqrt{\frac{\sigma \, \cos\theta}{2 \, \phi_i \, \eta}} \; \Gamma \; \sqrt{t} \tag{1}$$

and thus also for the sample's mass increase $m(t)$ due to the liquid uptake $m(t)$,

$$m(t) = \underbrace{A \, \rho \, \sqrt{\frac{\phi_i \, \sigma \, \cos\theta}{2 \, \eta}} \; \Gamma}_{C_m} \; \sqrt{t} \tag{2}$$

where the proportionality constant becomes:

$$\Gamma = \frac{r_h^2}{r_0} \sqrt{\frac{\phi_0}{\tau \, r_L}} \tag{3}$$

In the prefactor C_m of Eq. 2 σ, η, ρ, A refer to the surface tension, the shear viscosity, the density of the imbibing liquid, and the cross-sectional area A of the sample in contact with the bulk liquid reservoir, respectively. The contact angle θ describes the wettability of the pore wall by the liquid. The tortuosity $\tau = 3.6$ describes the connectivity and meandering of the pores in Vycor glasses (Gruener et al. 2016a; Lin et al. 1992). Moreover, we introduce the quantity Γ and term it Lucas–Washburn–Darcy imbibition ability. It is solely determined by matrix-specific quantities. Thus, it should be equal for matrices with identical internal structure and chemical composition – independent of the imbibed liquid. It can be considered as a generalized prefactor of the Lucas–Washburn law and thus of the imbibition speed. The larger Γ the faster is the imbibition process. It is directly proportional to the square root of the pore dimensions expressed by a pore radius r (as can be easily seen by applying $r_h = r_0 = r_L \equiv r$). Hence, the liquid will rise faster in larger pores.

The imbibition ability allows one to directly compare imbibition experiments with different liquids (Gruener et al. 2016a, b). Furthermore, its absolute value contains information on the nanoscopic flow behavior, especially on the hydrodynamic radius r_h and hence on the hydrodynamic boundary condition, which itself depends on the fluid/pore wall interaction.

4 Experimental Results and Discussion

The gravimetric experiments are illustrated by a representative mass increase measurement depicted in Fig. 3 for DC704 in V5. Four distinct regimes are observable. In the beginning, the sample hangs freely above the bulk reservoir, $m(t)=0$. The measurement is started by moving the cell upward until the sample touches the liquid surface. A liquid meniscus forms at the outer perimeter of the sample rod, see picture in Fig. 1c. This induces a traction force F_S acting on the porous matrix's surface toward the reservoir. For a given perimeter length P of the meniscus, it is determined by $F_S = P \sigma \cos\theta_0$, which for $\theta_0 = 0°$ and the surface tension $\sigma \approx 33 \frac{mN}{m}$ of silicone oil $T = 20 \deg C$ results in $F_S \approx 0.7$ mN or, equivalently, in a mass jump of $\Delta m \approx 0.07$ g, in good agreement with the measurement.

This mass jump is a constant offset that does not affect the subsequent imbibition process. The latter is the outstanding effect in regime (b) and can also nicely be tracked by optical imaging, see the picture in Fig. 1 and the movie on the imbibition process in the supplemental. There is a difference in the optical refractive index between the oil filled and the empty porous glass. This results in changes in the light refraction at the advancing imbibition front. In combination with the cylindrical matrix shape, this leads to an apparent macroscopic meniscus at the advancing oil front in an optical imaging experiment and thus allows one to track, in principle by bare eye, the imbibition front moving in the porous glass (Gruener 2010; Gruener et al. 2012, 2016a).

The mass uptake in regime (b) can be described by a $\sqrt{t}$-fit in accordance with Eq. (2), see Fig. 3. Thus, the $\sqrt{t}$-fit provides via Eq. (2) the imbibition ability. At some point, a plateau is reached (regime (c)) indicating that the sample is completely filled with liquid. The blue line in regime (d) finally indicates the overall mass uptake of the liquid saturated sample.

Analogous experiments are performed also for DC705 and V10 matrices, see Fig. 4 for the mass uptake of the corresponding liquid/matrix combination normalized by the cross-sectional area A of the Vycor monolith ($A_{V5} = 36.96$ mm^2, $A_{V10} = 25.23$ mm^2). The solid lines represent $\sqrt{t}$-fits. Except for an initial phase of a few minutes, where presumably due to the formation and slow relaxation of the meniscus at the outer perimeter of the sample as well as buoyancy effects due to the immersion in the viscous oils lead to deviations from
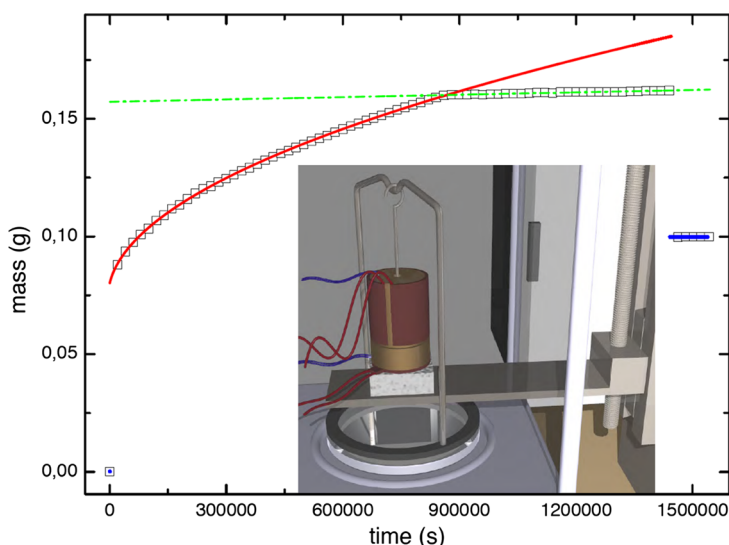
Fig. 3 Gravimetric imbibition experiment. Increase in mass (squares) of a porous Vycor block (V5) due to imbibition of silicone oil (DC704) at room temperature. According to Eq. (2), the prefactor of the $\sqrt{t}$-Lucas–Washburn–Darcy kinetics fit (red solid line) provides information on the microscopic flow behavior expressed in terms of the imbibition ability Γ. The mass increase comes to a halt and a constant plateau (dashed line) is reached, when the sample is completely filled. For clarity only every 1200th data point is shown. Inset: Gravimetric imbibition setup used for the capillary rise experiments (Gruener 2010; Gruener and Huber 2011)

the $\sqrt{t}$-scaling, the imbibition kinetics follows the Lucas–Washburn kinetics for several days. This evidences a remarkably robust description of the imbibition process by the L–W kinetics derived above. Except for the DC704/V10 and DC705/V5 systems which by coincidence almost agree in the imbibition dynamics, there are sizeable differences in the kinetics between the fluid/matrix combination resulting from the differing viscosities and mean hydraulic diameters. Note that in agreement with Eq. 3 the liquid uptake rate for a given pore diameter increases with decreasing viscosity and for a given viscosity with increasing pore diameter.

The $\sqrt{t}$-fits of the mass uptake curves, shown as solid lines in Fig. 4, result according to Eq. 2 in the imbibition coefficients $C_m = (7.6826 \pm 0.0009), (9.230 \pm 0.001), (3.2274 \pm 0.0016), (5.2958 \pm 0.0007) \cdot 10^{-5} g/\sqrt{s}$. Along with the bulk fluid properties, see Table 1, the cross-sectional areas of the V5 and V10 samples ($A_{V5} = 36.96$ mm^2, $A_{V10} = 25.23$ mm^2) and the initial porosities $\Phi_i = 0.275$ and 0.295 for V5 and V10, respectively, these experimentally determined values allow then to determine the corresponding imbibition abilities, *i.e.*, according to Eq. 2 $\Gamma = C_m/(A \rho \sqrt{\frac{\phi_i \sigma \cos\theta}{2\eta}})$. From these imbibition abilities the effective hydraulic radius r_h is determined with Eq. 2 and therefrom the slip lengths $b = r_h - r_0$, see Table 2 for the resulting imbibition abilities and slip lengths.

These slip lengths are all negative, indicating a reduced hydraulic radius r_h and thus indicate a sticking boundary layer, whose thickness is approximately 1.4 nm. The mean value determined from the four experiments is $\bar{b} = -(1.4 \pm 0.3)$ nm. Interestingly, this result is independent of both the sample type and the silicone oil. This encourages us to attribute this observation, similarly as in previous studies on water, hydrocarbon, and liquid crystal imbibition in silica (Gruener et al. 2009; Gruener and Huber 2009, 2011; Gruener

Table 2 Characterization of the imbibition dynamics of Dow Corning silicone oils in porous Vycor at room temperature by means of the imbibition ability Γ and the resultant slip length b

Liquid	Vycor V5		Vycor V10	
	Γ $(10^{-7}\sqrt{m})$	b (nm)	Γ $(10^{-7}\sqrt{m})$	b (nm)
DC704	63.6 ± 5.6	-1.35 ± 0.23	109.2 ± 12.6	-1.39 ± 0.40
DC705	53.2 ± 4.8	-1.52 ± 0.21	122.4 ± 11.4	-1.19 ± 0.38

et al. 2016a, b) to the formation of an immobile layer of strongly adsorbed molecules, that substantially lowers the invasion dynamics.

Arguably, the largest uncertainty in the determination of the slip length results from the ambiguities in the concept and the measurement of the tortuosity (Levitz 1998). To date, several techniques have been applied to extract the tortuosity of the isotropic pore network in Vycor glass. Deducing the diffusion coefficient of hexane and decane by means of small angle neutron scattering (SANS) measurements τ was found to be in the range of 3.4–4.2 (Lin et al. 1992). Calculations based on three-dimensional geometrical models for Vycor yielded a value of approximately 3.5 (Crossley et al. 1991; Levitz 1998). We chose a value of $\tau = 3.6$ with an uncertainty of ± 0.5. A tortuosity of about three seems reasonable if one considers that in an isotropic medium such as Vycor, the porosity can, in first approximation, be accounted for by three sets of parallel capillaries in the three spatial directions; but only one third of these capillaries sustain the flow along the pressure drop. Hence, the hydraulic permeability in the Darcy sense is reduced by a factor of 3. A value larger than three reflects the extended length of a meandering capillary beyond that of a straight one. According to Eq. 3 τ scales $\propto (r_0 + b)^4$ for a fixed Γ and mean radius. Thus, large uncertainties in τ result in comparably small changes in the slip lengths determined in our experiments, and, vice versa, small changes in the slip length b necessitate significantly altered τs. For example, to explain the measured Γs in our experiment with the standard no-slip boundary condition $b = 0$ (no sticky boundary layer), we would need $\tau = 27, 38, 13,$ and 11 to explain the Γs for the V5/DC704, V5/DC705, V10/DC704 and V10/DC705 fluid/matrix combinations, respectively. These values are unreasonable. Moreover, we would need for the identical sample type (V5 or V10) values which differ significantly as a function of employed silicone oil. By contrast, the consistent use of $\tau = 3.6 \pm 0.5$ for the analysis of all four fluid/pore radius combinations results in quite similar slip lengths, i.e., $\bar{b} = -(1.4 \pm 0.3)$ nm.

Note that Cai and Yu extended the classic Lucas–Washburn law toward the consideration of flow heterogeneity in porous media originating in the tortuosity of a porous medium (Cai and Yu 2011). This results in a modified time scaling of the invasion kinetics, $h(t) \propto t^{\frac{1}{2D_T}}$, where D_T is the fractal dimension of tortuosity in the Cai–Yu considerations with $1 < D_T < 3$. However, except for deviations in the initial imbibition times for the most viscous oil, which we trace to experimental artifacts related to the approach of the bulk reservoir, we observe a robust Lucas–Washburn kinetics, i.e., $D_T = 1$ for all fluid/media combinations studied here. Therefore, we conclude that in our experiments tortuosity-induced flow heterogeneities are negligible and the classic Lucas–Washburn law ($D_T = 1$) is valid.

At first glance, the oily character of the fluids employed may suggest a polymeric rheology, and thus one may have expected faster flow kinetics than predicted by a no-slip velocity boundary condition (Priezjev and Troian 2004; Dimitrov et al. 2007; Hatzikiriakos 2012), and thus positive slip lenghts. However, the molecular structure of the siloxanes studied here is not really flexible, chain-like but rather rigid, so that the observation of a negative slip length is not
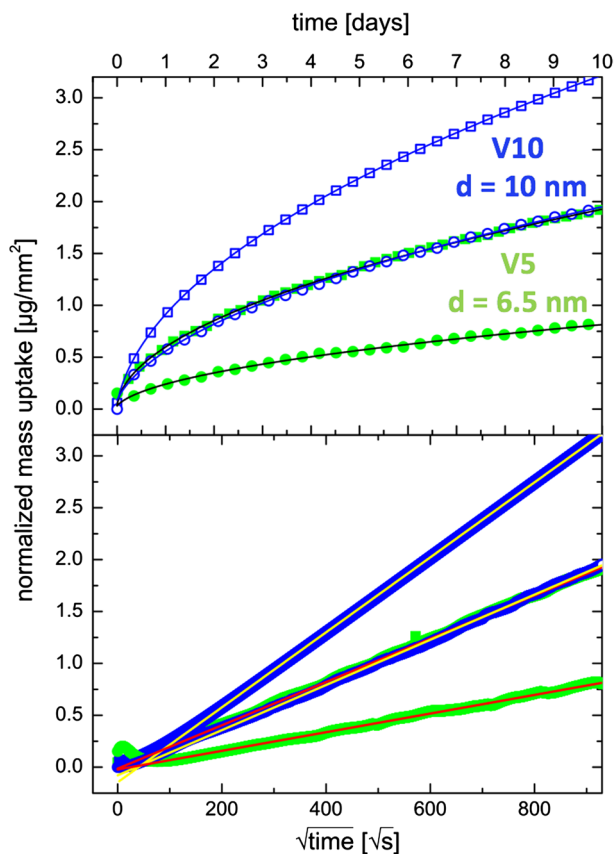
Fig. 4 Gravimetric experiment on silicone oil imbibition in monolithic nanoporous silica. **a** Plotted is the normalized mass uptake of Vycor glass V10 during imbibition of DC704 (open squares) and DC705 (open circles) as well as V5 upon DC704 (solid squares) and DC705 (solid circles) invasion, respectively. For clarity, only every 6000th data point is shown. The solid lines correspond to $\sqrt{t}$-fits of the capillary rise dynamics as discussed in the text. **b** Normalized mass uptakes of panel **a** versus $\sqrt{t}$. The straight lines represent $\sqrt{t}$-fits from which the imbibition abilities Γ are determined

too surprising. Moreover, in agreement with previous studies on simple wall-wetting liquids and thus strong attractive liquid–solid interaction sticky layers and thus negative bs, whereas for non-wetting situations rather positive and thus positive bs are expected (Vinogradova 1999; Lasne et al. 2008; Barrat and Bocquet 1999; Baeumchen et al. 2012; Wu et al. 2017a).

From previous analogous experiments on hydrophilic Vycor glasses (Gruener et al. 2009, 2016a) we suggest that independent of the respective silicone oil a monolayer of water directly adjacent to the pore walls is most likely an essential part of this sticking layer. The water coating of the pore walls is due to the finite humidity in our experiments of about 30%. It results in the formation of water layers adsorbed at the pore wall. Especially the first adsorbed water layer is stabilized by the attractive potential between the hydroxylated silica and the polar water molecules. This is also indicated by a pronounced monolayer step in sorption isotherms and a slow self-diffusion dynamics (Bonnaud et al. 2010) of water in hydroxylated nanopores. The sticky water layer is highly stabilized and cannot be displaced by the silicone molecules. It corresponds to a thickness of ~ 0.25 nm (Gruener et al. 2009). The remaining

part of the sticking layer thickness b can then be attributed to a second pinned layer composed of molecules of the silicone oils. Here, the block-like molecules are presumably arranged parallel to the pore walls (flat-lying), which results in an overall immobile boundary layer thickness of $\sim 1.4\,\text{nm} = (0.25 + 1.15)\,\text{nm}$, in good agreement with the negative bs observed.

For the mobile, inner region (away from the interface) classical concepts of hydrodynamics based on continuum-like properties such as shear viscosity and surface tension remain valid and we also find no hints for shear thinning or thickening. It would result in deviations from the $\sqrt{t}$-L–W dynamics (Cao et al. 2016), because of the variation of the shear rate during the imbibition process.

The partitioning in immobile interfacial liquid layers and bulk-like fluidity in the pore centers are also in accord with measurements on the self-diffusion dynamics of other, simple liquids in nanopores (Huber 2015). For example, one component with bulk-like self-diffusion dynamics and a second one which is immobile, and thus 'sticky', has been found in quasi-elastic neutron scattering experiments (Kusmin et al. 2010a, b; Hofmann et al. 2012).

The formation of layered structures of silicone oils at capillary walls has also been inferred from imbibition experiments performed for silicone oil in macroscopic borosilicate capillaries (Wu et al. 2017b). As discussed in detail in Wu et al. (2017b) it can result in sizeable changes in the contact angle as a function of the advancing menisci and thus to reduced imbibition velocities. Note, however, that here the meniscus velocities are orders of magnitude smaller than in macroscopic capillaries. Therefore, we assume unchanged contact angles close to 0 and trace the reduced imbibition velocities solely to the formation of an immobile boundary layer.

It is interesting to remark that a significant light scattering is observable at the invasion front, in particular in the late stages of the imbibition process after several days, see the imbibition video in the supplementary. As is outlined in detail in Gruener et al. (2016a) it can be traced to the disorder of the Vycor pore structure, in particular the pore size distribution. The resulting Laplace pressure and hydraulic permeability variations result in the formation of filled and still empty pore space volumes (Clotet et al. 2016), whose characteristic extensions are in the order of visible light wavelengths. Along with the difference in the refractive index between filled and empty pores, this leads to light scattering and thus in a whitening of the imbibition front. Neutron imaging experiments (Gruener et al. 2012, 2016a) in accord with pore network simulations and a scaling theory for the long time behavior of spontaneous imbibition in porous media consisting of interconnected pores with a large length-to-width ratio, as in Vycor, could trace the front broadening to a complex dynamics of the individual menisci. In particular long-lasting meniscus arrests, when at pore junctions the meniscus propagation in one or more branches comes to a halt when the Laplace pressure of the meniscus exceeds the hydrostatic pressure within the junction. Unfortunately, such single pore invasion events are not directly visualizable in nanoporous media so far, despite the substantial improvements in 3D X-ray tomography to resolve such events (Berg et al. 2013). However, microfluidic experiments corroborate the scenario (Sadjadi et al. 2015) outlined above.

Note, that the mean position of the imbibition front in Vycor is still well defined (Gruener et al. 2012, 2016a), despite the sizeable capillarity and permeability disorder, see Gruener et al. (2016a) for a detailed analysis of the imbibition front broadening for V5 and V10. Therefore, the measurement of the time-dependent gravimetric mass uptake, performed here, is a robust method to quantify the invasion kinetics in the complex, 3D interconnected pore network of Vycor glasses.

5 Conclusions

We experimentally explored spontaneous imbibition of silicone oils in mesoporous, monolithic silica glass. The kinetics follow Lucas–Washburn laws typical of spontaneous imbibition in macroporous media with homogeneous porosity. A Darcy analysis indicates that imbibition speeds can be quantitatively traced to bulk fluid parameters, if a sticking boundary layer of 1.4 nm of flat-lying silicone molecules and a monolayer of water adsorbed at the pore walls is assumed. These rheological insights are in good agreement with previous experiments on simple, wetting liquids in nanoporous media (Huber et al. 2007; Gruener et al. 2009; Gruener and Huber 2009, 2011; Gruener et al. 2016a; Vincent et al. 2016; Koklu et al. 2017). They are also corroborated by simulation studies on liquid transport in nanopores (Dimitrov et al. 2007; Vo et al. 2015; Vo and Kim 2016; Zhang 2018) and phenomenological models for spontaneous imbibition in nanoporous media (Shen et al. 2018; Feng et al. 2018).

Future studies on the polarity and hydration state-dependent flow across these silica monoliths would also be particularly interesting. These surface characteristics should have sizeable effects on the hydrodynamic boundary condition and eventually lead to a mobilization of the sticky boundary layer (Gruener et al. 2016a; Sendner et al. 2009). Also complementary measurements on the self-diffusion of the oil molecules, e.g., by quasi-elastic neutron scattering (Kusmin et al. 2010a, b) or nuclear magnetic resonance, (Valiullin et al. 2006) could give important information on the stochastic molecular motions and via the Stokes–Einstein relation on the flow viscosity in the spatially confined geometries.

The complex sponge-like geometry of our nanoporous media resemble on the one hand many technological and natural porous systems, on the other hand experiments on straight independent nanopores would reduce experimental ambiguities with regard to pore size distributions and tortuosity (Elizalde et al. 2014) and are thus desirable.

The pore space in tight oil reservoirs, in particular shale, can often roughly be segregated in inorganic hydrophilic pores and organic hydrophobic pores (Yassin et al. 2017; Zhang et al. 2018a). Even for macroscopic porosity, this dual-wettability results in particular complex front movements, where for example local instabilities control the progression of invading interfaces (Singh et al. 2017). In nanoporous systems the wettability-induced variation in hydrodynamic boundary conditions (negative and positive velocity slippage) could therefore induce even more complex front movement dynamics.

Also, multiscale porosity is present in many oil reservoirs, soils, rocks, and shales and materials such as concrete with a pore distribution spanning orders of magnitude, frequently from the macroscale down to sub-nm dimensions. Therefore, it would be also particularly interesting to explore spontaneous imbibition in sub-nm pores in the future. There, a non-Darcy behavior is expected (Falk et al. 2015), because of a complex interplay of adsorption, stochastic motions and viscous flow. Moreover, the advent of materials with well-defined hierarchical porosity (Hartmann and Schwieger 2016) may offer the possibility to explore multiscale descriptions of this complex interplay of transport mechanisms (Boţan et al. 2015).

References

Alyafei, N., Al-Menhali, A., Blunt, M.J.: Experimental and analytical investigation of spontaneous imbibition in water-wet carbonates. Transp. Porous Media **115**(1), 189–207 (2016). https://doi.org/10.1007/s11242-016-0761-4

Baeumchen, O., Fetzer, R., Klos, M., Lessel, M., Marquant, L., Haehl, H., Jacobs, K.: Slippage and nanorheology of thin liquid polymer films. J. Phys. Condens. Matter **24**(32), 325102 (2012). https://doi.org/10.1088/0953-8984/24/32/325102

Bao, B., Riordon, J., Mostowfi, F., Sinton, D.: Microfluidic and nanofluidic phase behaviour characterization for industrial CO_2, oil and gas. Lab On A Chip **17**(16), 2740–2759 (2017). https://doi.org/10.1039/c7lc00301c

Barrat, J., Bocquet, L.: Large slip effect at a nonwetting fluid–solid interface. Phys. Rev. Lett. **82**, 4671–4674 (1999)

Bell, J.M., Cameron, F.: The flow of liquids through capillary spaces. J. Phys. Chem. **10**, 658–674 (1906)

Berg, S., Ott, H., Klapp, S.A., Schwing, A., Neiteler, R., Brussee, N., Makurat, A., Leu, L., Enzmann, F., Schwarz, J.O., Kersten, M., Irvine, S., Stampanoni, M.: Real-time 3d imaging of haines jumps in porous media flow. Proc. Natl. Acad. Sci. U. S. A. **110**(10), 3755–3759 (2013). https://doi.org/10.1073/pnas.1221373110

Bocquet, L., Tabeling, P.: Physics and technological aspects of nanofluidics. Lab on a chip **14**(17), 3143–3158 (2014). https://doi.org/10.1039/c4lc00325j

Bonnaud, P.A., Coasne, B., Pellenq, R.J.M.: Molecular simulation of water confined in nanoporous silica. J. Phys. Condens. Matter **22**(28), 284110 (2010). https://doi.org/10.1088/0953-8984/22/28/284110

Boţan, A., Ulm, F.J., Pellenq, R.J.M., Coasne, B.: Bottom-up model of adsorption and transport in multiscale porous media. Phys. Rev. E **91**, 032133 (2015). https://doi.org/10.1103/PhysRevE.91.032133

Busch, M., Kityk, A.V., Piecek, W., Hofmann, T., Wallacher, D., Całus, S., Kula, P., Steinhart, M., Eich, M., Huber, P.: A ferroelectric liquid crystal confined in cylindrical nanopores: reversible smectic layer buckling, enhanced light rotation and extremely fast electro-optically active goldstone excitations. Nanoscale **9**(48), 19086–19099 (2017). https://doi.org/10.1039/C7NR07273B

Cai, J.C., Yu, B.M.: A discussion of the effect of tortuosity on the capillary imbibition in porous media. Transp. Porous Media **89**(2), 251–263 (2011). https://doi.org/10.1007/s11242-011-9767-0

Cao, B.Y., Yang, M., Hu, G.J.: Capillary filling dynamics of polymer melts in nanopores: experiments and rheological modelling. Rsc Adv. **6**(9), 7553–7559 (2016). https://doi.org/10.1039/c5ra24991k

Cieplak, M., Koplik, J., Banavar, J.R.: Boundary conditions at a fluid–solid interface. Phys. Rev. Lett. **86**, 803–806 (2001). https://doi.org/10.1103/PhysRevLett.86.803

Clotet, X., Santucci, S., Ortín, J.: Experimental study of stable imbibition displacements in a model open fracture. II. Scale-dependent avalanche dynamics. Phys. Rev. E **93**, 012150 (2016). https://doi.org/10.1103/PhysRevE.93.012150

Crossley, R.A., Schwartz, L.M., Banavar, J.R.: Image-based models of porous media: application to Vycor glass and carbonate rocks. Appl. Phys. Lett. **59**, 3553–3555 (1991)

Debye, P., Cleland, R.L.: Flow of liquid hydrocarbons in porous Vycor. J. Appl. Phys. **30**(6), 843–849 (1959)

de Jongh, P.E., Eggenhuisen, T.M.: Melt infiltration: an emerging technique for the preparation of novel functional nanostructured materials. Adv. Mater. **25**(46), 6672–6690 (2013). https://doi.org/10.1002/adma.201301912

Dimitrov, D., Milchev, A., Binder, K.: Capillary rise in nanopores: molecular dynamics evidence for the Lucas–Washburn equation. Phys. Rev. Lett. **99**, 054501 (2007)

Eijkel, J.C.T., van den Berg, A.: Nanofluidics: what is it and what can we expect from it? Nano Microfluid. **1**, 249–267 (2005)

Elizalde, E., Urteaga, R., Koropecki, R.R., Berli, C.L.A.: Inverse problem of capillary filling. Phys. Rev. Lett. **112**, 134502 (2014). https://doi.org/10.1103/PhysRevLett.112.134502

Falk, K., Coasne, B., Pellenq, R., Ulm, F.J., Bocquet, L.: Subcontinuum mass transport of condensed hydrocarbons in nanoporous media. Nat. Commun. **6**, 6949 (2015). https://doi.org/10.1038/ncomms7949

Feng, D., Li, X.F., Wang, X.Z., Li, J., Zhang, X.: Capillary filling under nanoconfinement: the relationship between effective viscosity and water–wall interactions. Int. J. Heat Mass Transf. **118**, 900–910 (2018). https://doi.org/10.1016/j.ijheatmasstransfer.2017.11.049

Gommes, C.J.: Stochastic models of disordered mesoporous materials for small-angle scattering analysis and more. Microporous Mesoporous Mater. **257**, 62–78 (2018). https://doi.org/10.1016/j.micromeso.2017.08.009

Gor, G.Y., Huber, P., Bernstein, N.: Adsorption-induced deformation of nanoporous materials—a review. Appl. Phys. Rev. **4**(1), 011303 (2017). https://doi.org/10.1063/1.4975001

Gor, G.Y., Huber, P., Weissmueller, J.: Elastocapillarity in nanopores: sorption strain from the actions of surface tension and surface stress. Phys. Rev. Mater. (2018) (**in press**)

Gruener, S.: Rheology and dynamics of simple and complex liquids in mesoporous matrices. Ph.D. thesis, Saarland University, Saarbruecken (2010)

Gruener, S., Huber, P.: Knudsen diffusion in silicon nanochannels. Phys. Rev. Lett. **100**, 064502 (2008)

Gruener, S., Huber, P.: Spontaneous imbibition dynamics of an n-alkane in nanopores: evidence of meniscus freezing and monolayer sticking. Phys. Rev. Lett. **103**, 174501 (2009)

Gruener, S., Huber, P.: Imbibition in mesoporous silica: rheological concepts and experiments on water and a liquid crystal. J. Phys. Condens. Matter **23**(18), 184109 (2011). https://doi.org/10.1088/0953-8984/23/18/184109

Gruener, S., Hofmann, T., Wallacher, D., Kityk, A.V., Huber, P.: Capillary rise of water in hydrophilic nanopores. Phys. Rev. E **79**, 067301 (2009)

Gruener, S., Sadjadi, Z., Hermes, H.E., Kityk, A.V., Knorr, K., Egelhaaf, S.U., Rieger, H., Huber, P.: Anomalous front broadening during spontaneous imbibition in a matrix with elongated pores. Proc. Natl. Acad. Sci. U. S. A. **109**(26), 10245–10250 (2012). https://doi.org/10.1073/pnas.1119352109

Gruener, S., Hermes, H.E., Schillinger, B., Egelhaaf, S.U., Huber, P.: Capillary rise dynamics of liquid hydrocarbons in mesoporous silica as explored by gravimetry, optical and neutron imaging: nano-rheology and determination of pore size distributions from the shape of imbibition fronts. Colloids Surf. A Physicochem. Eng. Asp. **496**, 13–27 (2016a). https://doi.org/10.1016/j.colsurfa.2015.09.055

Gruener, S., Wallacher, D., Greulich, S., Busch, M., Huber, P.: Hydraulic transport across hydrophilic and hydrophobic nanopores: flow experiments with water and n-hexane. Phys. Rev. E **93**(013102), 013102 (2016b). https://doi.org/10.1103/PhysRevE.93.013102

Hartmann, M., Schwieger, W.: Hierarchically-structured porous materials: from basic understanding to applications. Chem. Soc. Rev. **45**, 3311–3312 (2016). https://doi.org/10.1039/C6CS90043G

Hatzikiriakos, S.G.: Wall slip of molten polymers. Prog. Polym. Sci. (Oxf.) **37**(4), 624–643 (2012). https://doi.org/10.1016/j.progpolymsci.2011.09.004

Hofmann, T., Wallacher, D., Mayorova, M., Zorn, R., Frick, B., Huber, P.: Molecular dynamics of n-hexane: a quasi-elastic neutron scattering study on the bulk and spatially nanochannel-confined liquid. J. Chem. Phys. **136**(12), 124505 (2012). https://doi.org/10.1063/1.3696684

Holt, J.K., Park, H.G., Wang, Y.M., Stadermann, M., Artyukhin, A.B., Grigoropoulos, C.P., Noy, A., Bakajin, O.: Fast mass transport through sub-2-nanometer carbon nanotubes. Science **312**, 1034–1037 (2006)

Huber, P.: Soft matter in hard confinement: phase transition thermodynamics, structure, texture, diffusion and flow in nanoporous media. J. Phys. Condens. Matter **27**, 103102 (2015)

Huber, P., Knorr, K.: Adsorption–desorption isotherms and x-ray diffraction of Ar condensed into a porous glass matrix. Phys. Rev. B **60**, 12657–12665 (1999)

Huber, P., Gruener, S., Schaefer, C., Knorr, K., Kityk, A.V.: Rheology of liquids in nanopores: a study on the capillary rise of water, n-hexadecane and n-tetracosane in mesoporous silica. Eur. Phys. J. Spec. Top. **141**, 101–105 (2007)

Kelly, S., Torres-Verdin, C., Balhoff, M.T.: Influences of polarity and hydration cycles on imbibition hysteresis in silica nanochannels. Phys. Chem. Chem. Phys. **20**(1), 456–466 (2018). https://doi.org/10.1039/c7cp05833k

Kiepsch, S., Pelster, R.: Interplay of vapor adsorption and liquid imbibition in nanoporous vycor glass. Phys. Rev. E **93**(4), 043128 (2016). https://doi.org/10.1103/PhysRevE.93.043128

Kirby, B.: Micro- and Nanoscale Fluid Mechanics: Transport in Microfluidic Devices. Cambridge University Press, Cambridge (2010)

Koklu, A., Li, J.N., Sengor, S., Beskok, A.: Pressure-driven water flow through hydrophilic alumina nanomembranes. Microfluid. Nanofluid. **21**(7), 124 (2017). https://doi.org/10.1007/s10404-017-1960-1

Kornev, K.G., Neimark, A.V.: Spontaneous penetration of liquids into capillaries and porous membranes revisited. J. Colloid Interface Sci. **235**(1), 101–113 (2001). https://doi.org/10.1006/jcis.2000.7374

Kriel, F.H., Sedev, R., Priest, C.: Capillary filling of nanoscale channels and surface structure. Isr. J. Chem. **54**(11–12), 1519–1532 (2014). https://doi.org/10.1002/ijch.201400086

Kuijpers, C.J., van Stiphout, T.A.P., Huinink, H.P., Tomozeiu, N., Erich, S.J.F., Adan, O.C.G.: Quantitative measurements of capillary absorption in thin porous media by the automatic scanning absorptometer. Chem. Eng. Sci. **178**, 70–81 (2018). https://doi.org/10.1016/j.ces.2017.12.024

Kusmin, A., Gruener, S., Henschel, A., Holderer, O., Allgaier, J., Richter, D., Huber, P.: Evidence of a sticky boundary layer in nanochannels: a neutron spin echo study of n-hexatriacontane and poly(ethylene oxide) confined in porous silicon rid b-7690-2008. J. Phys. Chem. Lett. **1**(20), 3116–3121 (2010a). https://doi.org/10.1021/jz1012406

Kusmin, A., Gruener, S., Henschel, A., de Souza, N., Allgaier, J., Richter, D., Huber, P.: Polymer dynamics in nanochannels of porous silicon: a neutron spin echo study. Macromolecules **43**(19), 8162–8169 (2010b). https://doi.org/10.1021/ma1004925

Kvick, M., Martinez, D.M., Hewitt, D.R., Balmforth, N.J.: Imbibition with swelling: capillary rise in thin deformable porous media. Phys. Rev. Fluids **2**, 074001 (2017). https://doi.org/10.1103/PhysRevFluids.2.074001

Lasne, D., Maali, A., Amarouchene, Y., Cognet, L., Lounis, B., Kellay, H.: Velocity profiles of water flowing past solid glass surfaces using fluorescent nanoparticles and molecules as velocity probes. Phys. Rev. Lett. **100**, 214502 (2008)

Levitz, P.: Off-lattice reconstruction of porous media: critical evaluation, geometrical confinement and molecular transport. Adv. Colloids Interface Sci. **76**, 71–106 (1998)

Levitz, P., Ehret, G., Sinha, S., Drake, J.: Porous Vycor glass: the microstructure as probed by electron microscopy, direct energy transfer, small-angle scattering, and molecular adsorption. J. Chem. Phys. **95**, 6151–6161 (1991)

Li, Z., Seker, E.: Configurable microfluidic platform for investigating therapeutic delivery from biomedical device coatings. Lab Chip **17**, 3331–3337 (2017). https://doi.org/10.1039/C7LC00851A

Lin, M.Y., Abeles, B., Huang, J.S., Stasiewski, H.E., Zhang, Q.: Visocus flow and diffusion of liquids in microporous glasses. Phys. Rev. B **46**, 10701 (1992)

Lucas, R.: U"ber das Zeitgesetz des kapillaren Aufstiegs von Flüssigkeiten. Kolloid Zeitschrift **23**, 15–22 (1918)

Martin, J., Martin-Gonzalez, M., Francisco Fernandez, J., Caballero-Calero, O.: Ordered three-dimensional interconnected nanoarchitectures in anodic porous alumina. Nat. Commun. **5**, 5130 (2014). https://doi.org/10.1038/ncomms6130

Meng, Q., Liu, H., Wang, J.: A critical review on fundamental mechanisms of spontaneous imbibition and the impact of boundary condition, fluid viscosity and wettability. Adv. Geo-Energy Res. **1**, 1–17 (2017)

Montemore, M.M., Montessori, A., Succi, S., Barroo, C., Falcucci, G., Bell, D.C., Kaxiras, E.: Effect of nanoscale flows on the surface structure of nanoporous catalysts. J. Chem. Phys. **146**(21), 214703 (2017). https://doi.org/10.1063/1.4984614

Neto, C., Evans, D.R., Bonaccurso, E., Butt, H.J., Craig, V.S.J.: Boundary slip in Newtonian liquids: a review of experimental studies. Rep. Prog. Phys. **68**, 2859–2897 (2005)

Nordberg, M.E.: Properties of some vycor-brand glasses. J. Am. Ceram. Soc. **27**, 299–305 (1944)

Ortiz-Young, D., Chiu, H.C., Kim, S., Voïtchovsky, K., Riedo, E.: The interplay between apparent viscosity and wettability in nanoconfined water. Nat. Commun. **4**, 2482 (2013). https://doi.org/10.1038/ncomms3482

Persson, F., Thamdrup, L.H., Mikkelsen, M.B.L., Jaarlgard, S.E., Skafte-Pedersen, P., Bruus, H., Kristensen, A.: Double thermal oxidation scheme for the fabrication of SiO_2 nanochannels. Nanotechnology **18**(24), 245301 (2007). https://doi.org/10.1088/0957-4484/18/24/245301

Piruska, A., Gong, M., Sweedler, J.V., Bohn, P.W.: Nanofluidics in chemical analysis. Chem. Soc. Rev. **39**(3), 1060–1072 (2010). https://doi.org/10.1039/b900409m

Priezjev, N.V., Troian, S.M.: Molecular origin and dynamic behavior of slip in sheared polymer films. Phys. Rev. Lett. **92**, 018302 (2004)

Rideal, E.K.: On the flow of liquids under capillary pressure. Philos. Mag. **44**, 1152–1159 (1922)

Sadjadi, Z., Jung, M., Seemann, R., Rieger, H.: Meniscus arrest during capillary rise in asymmetric microfluidic pore junctions. Langmuir **31**(8), 2600–2608 (2015). https://doi.org/10.1021/la504149r

Schmatko, T., Hervet, H., Leger, L.: Friction and slip at simple fluid–solid interfaces: the roles of the molecular shape and the solid–liquid interaction. Phys. Rev. Lett. **94**, 244501 (2005)

Schmid, K.S., Geiger, S.: Universal scaling of spontaneous imbibition for arbitrary petrophysical properties: water-wet and mixed-wet states and handy's conjecture. J. Petrol. Sci. Eng. **101**, 44–61 (2013). https://doi.org/10.1016/j.petrol.2012.11.015

Schoch, R.B., Han, J., Renaud, P.: Transport phenomena in nanofluidics. Rev. Mod. Phys. **80**, 839–883 (2008)

Secchi, E., Marbach, S., Nigues, A., Stein, D., Siria, A., Bocquet, L.: Massive radius-dependent flow slippage in carbon nanotubes. Nature **537**(7619), 210–213 (2016). https://doi.org/10.1038/nature19315

Sendner, C., Horinek, D., Bocquet, L., Netz, R.R.: Interfacial water at hydrophobic and hydrophilic surfaces: slip, viscosity, and diffusion. Langmuir **25**(18), 10768–10781 (2009). https://doi.org/10.1021/la901314b

Sentker, K., Zantop, A.W., Lippmann, M., Hofmann, T., Seeck, O.H., Kityk, A.V., Yildirim, A., Schönhals, A., Mazza, M.G., Huber, P.: Quantized self-assembly of discotic rings in a liquid crystal confined in nanopores. Phys. Rev. Lett. **120**, 067801 (2018). https://doi.org/10.1103/PhysRevLett.120.067801

Servantie, J., Mueller, M.: Temperature dependence of the slip length in polymer melts at attractive surfaces. Phys. Rev. Lett. **101**(2), 026101 (2008). https://doi.org/10.1103/PhysRevLett.101.026101

Shen, A., Xu, Y., Liu, Y., Cai, B., Liang, S., Wang, F.: A model for capillary rise in micro-tube restrained by a sticky layer. Results Phys. **9**, 86–90 (2018). https://doi.org/10.1016/j.rinp.2018.02.026. http://www.sciencedirect.com/science/article/pii/S2211379717325457

Shin, K., Obukhov, S., Chen, J.T., Huh, J., Hwang, Y., Mok, S., Dobriyal, P., Thiyagarajan, P., Russell, T.P.: Enhanced mobility of confined polymers. Nat. Mater. **6**, 961–965 (2007)

Singh, K., Scholl, H., Brinkmann, M., Michiel, M.D., Scheel, M., Herminghaus, S., Seemann, R.: The role of local instabilities in fluid invasion into permeable media. Sci. Rep. **7**(1), 444 (2017). https://doi.org/10.1038/s41598-017-00191-y

Sousa, C.T., Leitao, D.C., Proenca, M.P., Ventura, J., Pereira, A.M., Araujo, J.P.: Nanoporous alumina as templates for multifunctional applications. Appl. Phys. Rev. **1**(3), 031102 (2014). https://doi.org/10.1063/1.4893546

Squires, T.M., Quake, S.R.: Microfluidics: fluid physics at the nanoliter scale. Rev. Mod. Phys. **77**, 977–1026 (2005)

Stone, H.A., Stroock, A.D., Ajdari, A.: Engineering flows in small devices: microfluidics toward a lab-on-a-chip. Annu. Rev. Fluid Mech. **36**, 381–411 (2004). https://doi.org/10.1146/annurev.fluid.36.050802.122124

Stroock, A.D., Pagay, V.V., Zwieniecki, M.A., Holbrook, N.M.: The physicochemical hydrodynamics of vascular plants. Annu. Rev. Fluid Mech. **46**(46), 615–642 (2014). https://doi.org/10.1146/annurev-fluid-010313-141411

Thompson, P.A., Troian, S.M.: A general boundary condition for liquid flow at solid surfaces. Nature **389**, 360 (1997). https://doi.org/10.1038/38686

Valiullin, R., Naumov, S., Galvosas, P., Kaerger, J., Woo, H.J., Porcheron, F., Monson, P.A.: Exploration of molecular dynamics during transient sorption of fluids in mesoporous materials. Nature **443**(7114), 965–968 (2006). https://doi.org/10.1038/nature05183

Vincent, O., Szenicer, A., Stroock, A.D.: Capillarity-driven flows at the continuum limit. Soft Matter **12**(31), 6656–6661 (2016). https://doi.org/10.1039/c6sm00733c

Vincent, O., Marguet, B., Stroock, A.D.: Imbibition triggered by capillary condensation in nanopores. Langmuir **33**(7), 1655–1661 (2017). https://doi.org/10.1021/acs.langmuir.6b04534

Vinogradova, O.: Slippage of water over hydrophobic surfaces. Int. J. Miner. Process. **56**, 31–60 (1999)

Vo, T.Q., Kim, B.: Transport phenomena of water in molecular fluidic channels. Sci. Rep. **6**, 33881 (2016). https://doi.org/10.1038/srep33881

Vo, T.Q., Barisik, M., Kim, B.: Near-surface viscosity effects on capillary rise of water in nanotubes. Phys. Rev. E **92**(5), 053009 (2015). https://doi.org/10.1103/PhysRevE.92.053009

Wang, S., Feng, Q., Javadpour, F., Yang, Y.B.: Breakdown of fast mass transport of methane through calcite nanopores. J. Phys. Chem. C **120**(26), 14260–14269 (2016). https://doi.org/10.1021/acs.jpcc.6b05511

Washburn, E.: The dynamics of capillary flow. Phys. Rev. **17**, 273–283 (1921)

Wohlfarth, C., Wohlfarth, B.: Surface Tension of Pure Liquids and Binary Liquid Mixtures, Landolt-Börnstein—Group IV Physical Chemistry: Numerical Data and Functional Relationships in Science and Technology, vol. 16. Springer, Berlin (1997)

Wu, K.L., Chen, Z.X., Li, J., Li, X.F., Xu, J.Z., Dong, X.H.: Wettability effect on nanoconfined water flow. Proc. Natl. Acad. Sci. U. S. A. **114**(13), 3358–3363 (2017a). https://doi.org/10.1073/pnas.1612608114

Wu, P., Nikolov, A.D., Wasan, D.T.: Capillary rise: validity of the dynamic contact angle models. Langmuir **33**(32), 7862–7872 (2017b). https://doi.org/10.1021/acs.langmuir.7b01762. **PMID: 28722421**

Xue, Y.H., Markmann, J., Duan, H.L., Weissmuller, J., Huber, P.: Switchable imbibition in nanoporous gold. Nat. Commun. **5**, 4237 (2014)

Yamashita, K., Daiguji, H.: Molecular dynamics simulations of water uptake into a silica nanopore. J. Phys. Chem. C **119**(6), 3012–3023 (2015). https://doi.org/10.1021/jp5088493

Yang, S., Dehghanpour, H., Binazadeh, M., Dong, P.C.: A molecular dynamics explanation for fast imbibition of oil in organic tight rocks. Fuel **190**, 409–419 (2017). https://doi.org/10.1016/j.fuel.2016.10.105

Yao, Y., Alexandris, S., Henrich, F., Auernhammer, G., Steinhart, M., Butt, H.J., Floudas, G.: Complex dynamics of capillary imbibition of poly(ethylene oxide) melts in nanoporous alumina. J. Chem. Phys. **146**(20), 203320 (2017). https://doi.org/10.1063/1.4978298

Yassin, M.R., Begum, M., Dehghanpour, H.: Organic shale wettability and its relationship to other petrophysical properties: a duvernay case study. Int. J. Coal Geol. **169**(Complete), 74–91 (2017). https://doi.org/10.1016/j.coal.2016.11.015

Zhang, Y.: Size effect on nanochannel flow explored by the flow factor approach model. Int. J. Heat Mass Transf. **125**, 681–685 (2018). https://doi.org/10.1016/j.ijheatmasstransfer.2018.04.064. https://www.sciencedirect.com/science/article/pii/S0017931017354856

Zhang, T., Li, X.F., Li, J., Feng, D., Wu, K.L., Shi, J.T., Sun, Z., Han, S.: A fractal model for gas-water relative permeability in inorganic shale with nanoscale pores. Transp. Porous Media **122**(2), 305–331 (2018a). https://doi.org/10.1007/s11242-018-1006-5

Zhang, Z., Wen, L.P., Jiang, L.: Bioinspired smart asymmetric nanochannel membranes. Chem. Soc. Rev. **47**(2), 322–356 (2018b). https://doi.org/10.1039/c7cs00688h

Zhou, M., Caré, S., Courtier-Murias, D., Faure, P., Rodts, S., Coussot, P.: Magnetic resonance imaging evidences of the impact of water sorption on hardwood capillary imbibition dynamics. Wood Sci. Technol. **52**, 929–955 (2018). https://doi.org/10.1007/s00226-018-1017-y